

Mr. DETR: Instructive Multi-Route Training for Detection Transformers

Chang-Bin Zhang¹Yujie Zhong²Kai Han^{1†}¹Visual AI Lab, The University of Hong Kong²Meituan Inc.

Abstract

Existing methods enhance the training of detection transformers by incorporating an auxiliary one-to-many assignment. In this work, we treat the model as a multi-task framework, simultaneously performing one-to-one and one-to-many predictions. We investigate the roles of each component in the transformer decoder across these two training targets, including self-attention, cross-attention, and feed-forward network. Our empirical results demonstrate that any independent component in the decoder can effectively learn both targets simultaneously, even when other components are shared. This finding leads us to propose a multi-route training mechanism, featuring a primary route for one-to-one prediction and two auxiliary training routes for one-to-many prediction. We enhance the training mechanism with a novel instructive self-attention that dynamically and flexibly guides object queries for one-to-many prediction. The auxiliary routes are removed during inference, ensuring no impact on model architecture or inference cost. We conduct extensive experiments on various baselines, achieving consistent improvements as shown in Fig. 1.

1. Introduction

The end-to-end detection transformer (DETR) [3], along with subsequent studies [33, 40, 50], shine in object detection due to its simplicity and effectiveness. Unlike traditional methods, DETR-based detectors eliminate the need for post-processing steps like non-maximum-suppression (NMS). They employ the one-to-one assignment strategy (see Fig. 2(a)) for supervision, where each ground-truth box is matched to a single prediction. Compared to the one-to-many assignment methods (see Fig. 2(b)) in conventional object detectors [32, 43, 49] that allow each ground-truth box to be assigned with multiple predictions, the one-to-one assignment can lead to slow convergence [20, 47, 58] of DETRs due to its sparse supervision.

To accelerate the training of DETR-like object detectors,

[†]Corresponding author.

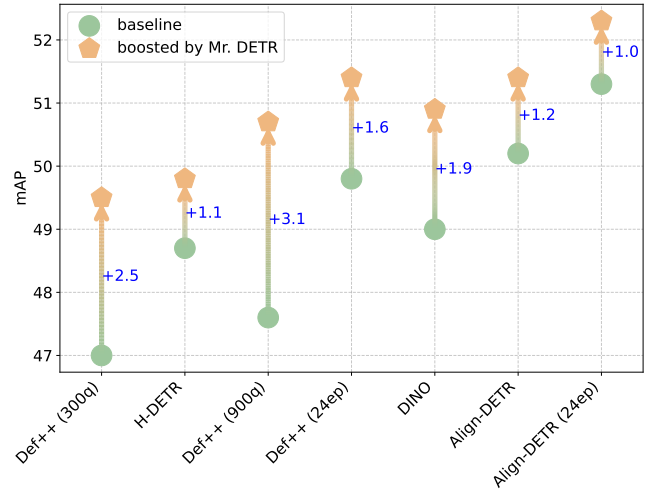


Figure 1. **Improvements over different baseline models.** The results are reported on the COCO 2017 validation in mean Average Precision (mAP). From left to right: Deformable-DETR++ [67] with 300 queries, H-DETR [20], Deformable-DETR++ [67] with 900 queries, Deformable-DETR++ [67] trained for 24 epochs, DINO [58], Align-DETR [1] and Align-DETR [1] configured with 24 training epochs.

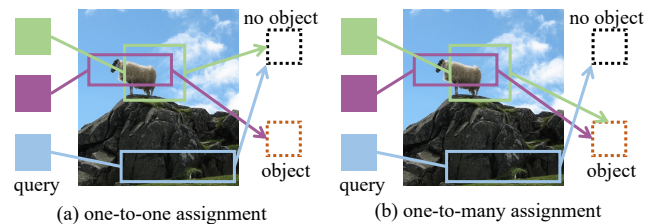


Figure 2. **One-to-one vs. one-to-many assignments.** (a) ‘One-to-one’ assigns each ground-truth box to a single predicted box, while predictions not associated with any object are supervised by ‘no object’ (background). (b) ‘One-to-many’ allows each ground-truth box to be paired with multiple predicted boxes.

several works propose auxiliary training methods to improve the quality of prediction localization by introducing auxiliary one-to-many assignment [19, 20, 62] or multiple groups of one-to-one assignment [5, 26, 58]. Specifically, DN-DETR [26], Group-DETR, and DINO [58] utilize multiple groups of parallel auxiliary queries that share the same transformer decoder with the primary object query. DETA [41]

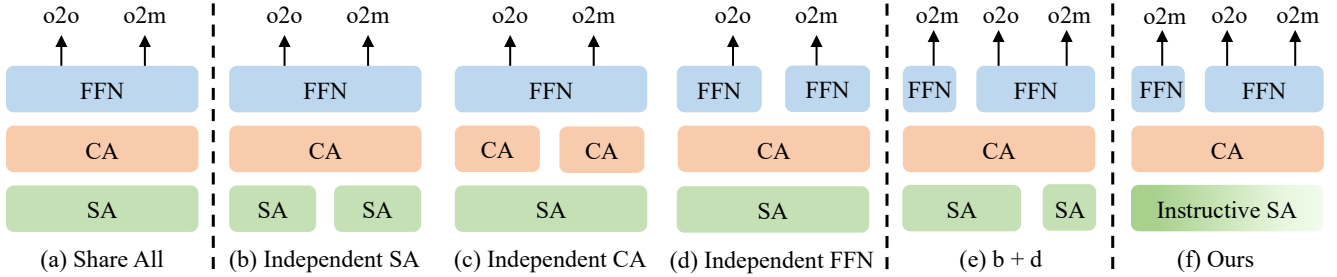


Figure 3. **Different configurations of the transformer decoder with auxiliary one-to-many training.** ‘SA’: self-attention. ‘CA’: cross-attention. ‘FFN’: feed-forward network. ‘o2o’: one-to-one prediction. ‘o2m’: one-to-many prediction.

No	Configurations	Routes	o2o	o2m
(1)	One-to-one only	1	47.6	-
(2)	Share All	1	41.6 (-6.0)	41.6
(3)	Not shared Self-Attention	2	49.7 (+2.1)	50.3
(4)	Not shared Cross-Attention	2	49.2 (+1.6)	50.0
(5)	Not shared FFN	2	49.6 (+2.0)	50.1
(6)	Shared Self-Attention	2	49.4 (+1.8)	50.3
(7)	Shared Cross-Attention	2	49.4 (+1.8)	50.0
(8)	Shared FFN	2	49.2 (+1.6)	50.0
(9)	(3) + (4)	3	49.4 (+1.8)	49.9
(10)	(3) + (5)	3	50.0 (+2.4)	50.8
(11)	(4) + (5)	3	49.0 (+1.4)	49.6
(12)	(3) + (4) + (5)	4	49.6 (+2.0)	50.2

Table 1. **The AP performance of different variants.** Each variant includes a primary route for one-to-one prediction and several auxiliary routes for one-to-many prediction. ‘o2o’: the performance of the primary route. ‘o2m’: the maximum performance with NMS among the auxiliary routes.

finds that self-attention is necessary when the model is required to conduct one-to-one prediction, but not when the model performs one-to-many prediction. Based on this observation, DAC-DETR [19] and MS-DETR [62] incorporate one-to-many auxiliary training by explicitly constraining self-attention and cross-attention to make the one-to-one and one-to-many prediction, respectively. We regard the model architecture that performs one-to-one and one-to-many prediction simultaneously as a multi-task framework. However, previous works examine the functions of each component in the transformer decoder for two training targets only in the single-task setting. A similar investigation in a multi-task framework still needs to be conducted in a rigorous way.

In this work, we first build the multi-task framework and empirically investigate the roles of each component in the transformer decoder for one-to-one and one-to-many assignments, including self-attention, cross-attention, and the feed-forward network (FFN). Specifically, we regard the model with auxiliary training by one-to-many assignment as a typical multi-task framework, requiring simultaneous one-to-one and one-to-many predictions. As illustrated in Fig. 3(a), the most straightforward approach is to obtain the prediction results of two tasks with shared components. However, ex-

perimental results in Tab. 1(1) indicate that *incorporating a one-to-many assignment significantly degrades the performance of the primary one-to-one prediction when all components are shared between two tasks*. Consequently, we investigate which component can be independent to enhance the primary route’s performance. We build the multi-task framework with independent self-attention, cross-attention, and FFN for two training targets, as shown in Fig. 3(b-d), respectively. We find that *any independent component significantly benefits the primary route of one-to-one prediction, even when other components are shared*, achieving 2.1%, 1.6%, and 2.0% improvement, respectively, as demonstrated in Tab. 1(3-5). We also explore the different auxiliary routes with two independent components, which show similar performance to those with a single independent component, but involve more trainable parameters. Therefore, we do not consider auxiliary training routes with two independent components.

This empirical finding motivates us to build a multi-route training mechanism that combines multiple auxiliary training routes, each with an independent component. Specifically, the primary route is used for the one-to-one prediction, while each auxiliary route features a distinct independent component for one-to-many prediction. For instance, in Fig. 3(e), we integrate auxiliary training using independent self-attention and FFN, respectively, with the primary route. We conduct experiments to verify the performance of each combination in Tab. 1. We find that when involving an auxiliary route with independent cross-attention degrades the primary route’s performance, likely due to the slow convergence [47] of independent cross-attention. The combination in Fig. 3(e) outperforms other variants, leading us to adopt this framework as our potential solution.

To further reduce the new trainable parameters in the auxiliary training routes and enhance parameter sharing across all routes, we propose a novel instructive self-attention mechanism, depicted in Fig. 3(f). Our approach includes three training routes, a primary route for one-to-one prediction, and two auxiliary routes with instructive self-attention and independent FFN, respectively. The first auxiliary route shares all parameters with the self-attention in the primary route, but incorporates a learnable token, named instruction token,

attached to the input object queries in the self-attention. The object queries, along with the instruction tokens, undergo self-attention, enabling the instruction token to guide the queries for one-to-many prediction. Given that the FFN is implemented as a simple two-layer MLP, we directly employ the independent FFN in the second auxiliary route. During inference, the two auxiliary training routes are discarded, ensuring the model architecture and inference time remain consistent with baseline models.

In summary, we make the following three contributions: *First*, in the multi-task framework, we empirically demonstrate that any independent component in the decoder can effectively learn one-to-one and one-to-many targets simultaneously, even when other components are shared. *Second*, building on the above insight, we propose a multi-route training mechanism and enhance it with our proposed instructive self-attention that dynamically and flexibly guides object queries for one-to-many prediction. *Third*, to verify the effectiveness of our method, we conduct extensive experiments on the COCO 2017 dataset, demonstrating consistent improvements across various baseline models.

2. Related Work

Detection with Transformers. Numerous follow-up works [9, 12, 67] accelerate the DETR [3] convergence by incorporating advanced attention architectures [13, 18, 36, 54, 56, 63, 67] or novel anchor box generation methods [17, 33, 40, 50, 53, 61]. Additionally, some studies propose lightweight detectors [6, 27, 30, 44, 64] or localization-aware objective [1, 18, 34, 42, 59]. In this work, we propose a multi-route training mechanism that enhances the training of DETR models while maintaining the original model architecture during inference.

Training Detection Transformers. Many typical object detectors [11, 15, 32, 43, 49, 60, 65] design various strategies to match each target with multiple predictions, thereby improving the detector’s ability to learn robust representations [20]. In contrast, DETR-like detectors [2, 3, 7, 14, 29, 52] achieve end-to-end object detection through one-to-one matching, where each target is assigned to a single prediction, considering both localization and classification costs. Nonetheless, DETR-like detectors with one-to-one matching frequently encounter slow convergence issues [20, 40, 47]. To accelerate the training of vanilla DETR [3], several studies incorporate auxiliary training methods. For instance, H-DETR [20] leverages Hungarian Matching [24] to construct one-to-many matching by duplicating targets. DN-DETR [26] and DINO [58] design multiple groups of denoising queries to accelerate the training of detection transformers. Likewise, Group-DETR [5] utilizes a set of learnable queries as the auxiliary input for the transformer decoder. DQ-DETR [8] establishes the primary query group by dynamically fusing auxiliary queries. StageInteractor [48] introduces one-to-

many matching by combining the label assignment results of different decoder layers. SQR-DETR [4] constructs auxiliary training by reusing object queries from previous decoder layers. Co-DETR [68] adopts multiple query groups with different matching strategies to offer various supervision signals. DAC-DETR [19] develops a parallel decoder to learn a one-to-many assignment by eliminating self-attention. MS-DETR [62] proposes to supervise cross-attention output using one-to-many matching, while self-attention is supervised by one-to-one matching.

3. Method

3.1. Preliminary

DETR Architecture. DETR-like detectors typically consist of an image backbone, transformer encoder, and decoder. The transformer encoder extracts features through self-attention among multi-scale image tokens. A set of object queries $\mathbf{Q} = \{q_0, q_1, \dots, q_n\}$ is fed into the transformer decoder, where classification and box regression heads derive the predicted classification $\mathbf{S} = \{s_0, s_1, \dots, s_n\}$ and bounding boxes $\mathbf{B} = \{b_0, b_1, \dots, b_n\}$ from the query output. The decoder consists of L stacked transformer layers, each containing self-attention, cross-attention, and a feed-forward network (FFN). Self-attention is applied between object queries, cross-attention facilitates interaction between object queries and image features, and the FFN extracts features in the object queries.

One-to-one Training Objective. Utilizing a one-to-one training objective [3], DETRs achieve end-to-end detection without the need for non-maximum-suppression (NMS). Specifically, let $\bar{\mathbf{B}} = \{\bar{b}_0, \bar{b}_1, \dots, \bar{b}_t\}$ and $\bar{\mathbf{S}} = \{\bar{s}_0, \bar{s}_1, \dots, \bar{s}_t\}$ represent the ground-truth boxes and corresponding classes. The matching cost between all possible prediction and ground-truth pairs is derived by considering both the classification cost and box costs. Optimal matches are determined using bipartite matching [3, 24], denoted as σ . The one-to-one training objective is expressed as:

$$L = \sum_{i=0}^t L_{cls}(s_{\sigma(i)}, \bar{s}_i) + L_{box}(b_{\sigma(i)}, \bar{b}_i), \quad (1)$$

where the L_{cls} and L_{box} represent the classification and bounding box losses, respectively.

One-to-many Training Objective. Traditional object detectors [32, 43, 49] typically use a one-to-many assignment strategy, assigning each ground truth box to multiple predictions based on specific criteria, followed by NMS to eliminate duplicated predictions. In our work, we apply a straightforward one-to-many assignment strategy [41] as in [19, 62], which considers localization quality and classification confidence, making it suitable for DETR-like detectors. Specifically, the matching score M_{ij} between the

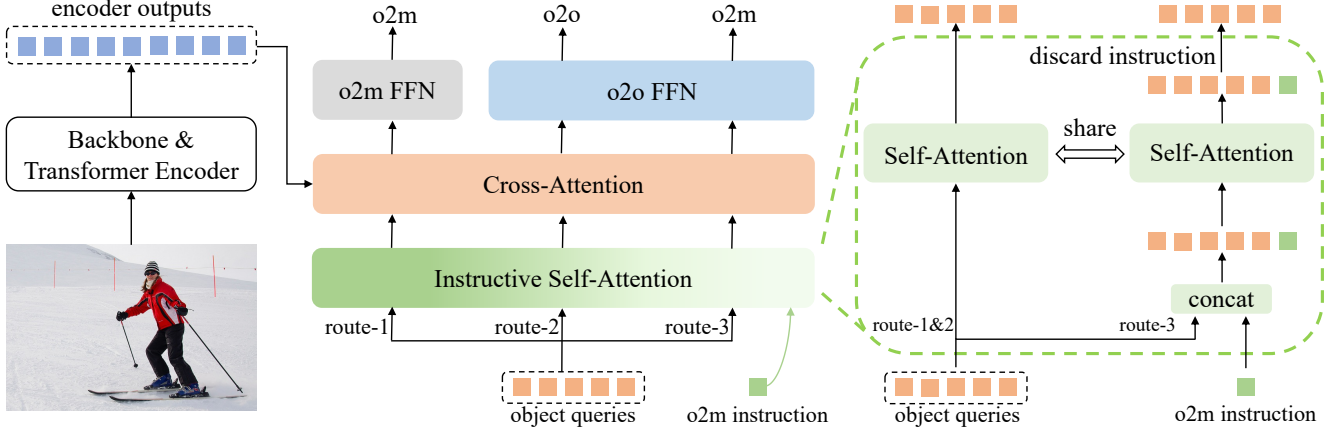


Figure 4. **Illustration of our proposed multi-route training method.** It includes three training routes: Route-1, Route-2, and Route-3. All three routes share the same object queries and detection heads for classification and regression. Route-2 serves as the primary route for one-to-one prediction, identical to the baseline models. Route-1 shares self-attention and cross-attention but uses an independent feed-forward network (o2m FFN) for one-to-many prediction. Route-3, sharing all components with the primary route, introduces a novel instructive self-attention, implemented by adding a learnable instruction token to the object queries to guide them and the subsequent network for one-to-many prediction. During inference, the auxiliary routes, Route-1 and Route-3, are discarded.

predictions (s_i, b_i) and the ground truth (\bar{s}_i, \bar{b}_i) is defined as:

$$M_{ij} = \alpha \cdot s_i + (1 - \alpha) \cdot \text{IoU}(b_i, \bar{b}_j), \quad (2)$$

where IoU computes the intersect-over-union between prediction box b_i and the ground-truth box \bar{b}_j . Given a maximum number of positive candidates K and an IoU threshold τ , positive predictions can be determined. First, up to K predictions with the highest matching scores M are selected as positive predictions. Then, for each ground-truth box, predictions with an IoU lower than τ are filtered out. The localization and classification losses are calculated as in Eqn. (1).

3.2. Multi-route Training

We aim to introduce the one-to-many assignment as an additional training strategy to enhance detection transformers. First, we treat the detector with auxiliary one-to-many prediction as a multi-task framework, which simultaneously achieves both one-to-one and one-to-many predictions. As discussed in Sec. 1, we empirically investigate the roles of each component in the transformer decoder within this framework and find: **(i)** incorporating a one-to-many assignment significantly degrades the performance of the primary one-to-one prediction when all components are shared between two tasks (see Tab. 1(2)). We anticipate that *it results from the interference between two tasks*. For instance, a predicted box may be assigned as a positive prediction in the one-to-many assignment, while being assigned as a negative prediction in the one-to-one assignment. **(ii)** any independent component in the decoder significantly benefits the primary one-to-one prediction route, even when other components are shared (see Fig. 3 (b - d) & Tab. 1 (3-5)). This observation indicates that *any independent component is capable of effec-*

tively mastering one-to-one and one-to-many training goals, thereby resolving the conflict between these two tasks. This is expected since shared components can extract common clues for two tasks, while independent components further distinguish different tasks; **(iii)** an auxiliary training route with two independent components does not outperform the route with only one independent component (see Tab. 1(6-8)); and **(iv)** combining the auxiliary route with independent self-attention and independent FFN achieves the highest performance among variants that combine different auxiliary training routes (see Tab. 1(10)).

Building on these findings, our method includes three training routes, as shown in Fig. 4. We share object queries, classification, and regression heads among the three routes. Route-2 is the primary route for one-to-one prediction, which is identical to baseline models. Route-1 and route-3 are auxiliary training routes used for one-to-many predictions, which are discarded during inference. Thus, the auxiliary training routes in our method do not affect model architecture or inference time.

Primary Route for One-to-one Prediction. The architecture and training objective of route-2 in Fig. 4 is the same as the baseline model. Specifically, for Route-2, given object queries $\mathbf{Q} = \{q_0, q_1, \dots, q_{n-1}\}$, the query output is defined as:

$$\hat{\mathbf{Q}}_2 = (\text{FFN}_{o2o} \circ \text{CA} \circ \text{SA})(\mathbf{Q}), \quad (3)$$

where SA, CA and FFN_{o2o} represent self-attention, cross-attention and FFN, respectively. The query output of Route-2 is supervised by one-to-one assignment in Eqn. (1). During inference, Route-2 is retained to achieve one-to-one prediction without any additional cost.

Auxiliary Route with Independent FFN. As depicted in Fig. 4, we integrate an auxiliary training route, re-

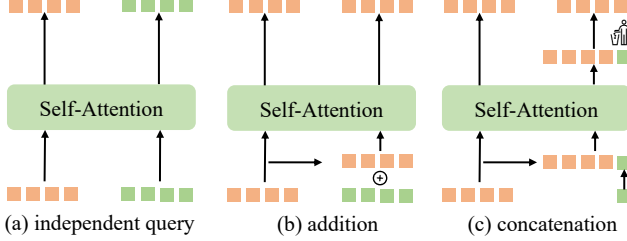


Figure 5. **Various implementations of instructive self-attention.**

ferred to as Route-1, featuring a separate FFN into our approach. Specifically, we directly employ an independent FFN, FFN_{o2m} in Route-1 sharing all self-attention and cross-attention components with the primary route. Due to the straightforward architecture and efficient parameter utilization of the FFN, we maintain its independence without further modification. The query output $\hat{\mathbf{Q}}_1$ of Route-1 can be written as:

$$\hat{\mathbf{Q}}_1 = (\text{FFN}_{o2m} \circ \text{CA} \circ \text{SA})(\mathbf{Q}). \quad (4)$$

This output is supervised by a one-to-many assignment.

Auxiliary Route with Instructive Self-Attention. In Sec. 1, we discuss the motivation for incorporating independent self-attention in Route-3 as shown in Fig. 3(e), designed for one-to-many prediction. To further reduce trainable parameters and enhance parameter sharing with the primary route, we propose an innovative instruction mechanism as shown in Fig. 4. This mechanism guides shared object queries to enable one-to-many prediction. The query output $\hat{\mathbf{Q}}_3$ of Route-3 is written as:

$$\hat{\mathbf{Q}}_3 = (\text{FFN}_{o2o} \circ \text{CA} \circ \text{InstructSA})(\mathbf{Q}), \quad (5)$$

where InstructSA denotes our proposed instructive self-attention which shares parameters with the self-attention in the other two routes. The output $\hat{\mathbf{Q}}_3$ is supervised by one-to-many assignment. Next, we will present the details of our instructive self-attention InstructSA design.

3.3. Instructive Self-Attention

As described in Sec. 3.2, Route-3 is realized using an instructive self-attention, which incorporates learnable instruction tokens \mathbf{Q}^{ins} into object queries \mathbf{Q} , creating a combined sequence $\hat{\mathbf{Q}}^{\text{ins}}$. Self-Attention is performed on this combined sequence. In this section, we examine distinct implementations of instructive self-attention aimed at informing object queries to realize one-to-many predictions, sharing self-attention parameters with the primary route. The simplest approach, depicted in Fig. 5(a), involves using a separate set of queries as inputs to facilitate one-to-many predictions. To improve the compatibility of object queries across different routes, we introduce learnable tokens that serve as instruction, delineating the prediction objectives. As depicted in Fig. 5(b), these instruction tokens are incorporated

into shared object queries through addition. This approach necessitates a fixed number of instruction tokens equivalent to the query count. Unlike the addition approach, our method adapts instruction tokens through concatenation, thereby providing greater flexibility. As illustrated in Fig. 5(c), this flexibility extends not just to the number of instruction tokens, but also allows these learned tokens to dynamically transmit information to object queries via self-attention. Self-attention is performed on the combined sequence $\hat{\mathbf{Q}}^{\text{ins}}$, but the corresponding outputs of the instructive tokens are discarded after self-attention because they are not intended for object localization. Further details can be found in Eqn. (6). In this way, the instruction tokens provide effective and adaptable guidance to Route-3, enabling it to make one-to-many predictions while utilizing shared parameters with the primary route. In Sec. 4.5, we evaluate the performance of various implementations.

Specifically, we build m learnable tokens $\mathbf{Q}^{\text{ins}} = \{q_0^{\text{ins}}, q_1^{\text{ins}}, \dots, q_{m-1}^{\text{ins}}\}$, called instruction tokens. Initially, these instruction tokens are attached to the input sequence of self-attention by concatenation, forming a composite set of input queries $\hat{\mathbf{Q}}^{\text{ins}} = \{q_0^{\text{ins}}, q_1^{\text{ins}}, \dots, q_{m-1}^{\text{ins}}, q_0, q_1, \dots, q_{n-1}\}$, resulting in a length of $m + n$. Subsequently, self-attention is performed on these combined queries. As the attached instruction tokens are not utilized for object localization, their outputs are discarded post self-attention, serving solely to convey information to object queries. The output $\hat{\mathbf{Q}}_3$ of Route-3 is written as:

$$\hat{\mathbf{Q}}_3 = (\text{FFN}_{o2o} \circ \text{CA} \circ \text{E} \circ \text{SA})(\hat{\mathbf{Q}}^{\text{ins}}), \quad (6)$$

where the function E eliminates the outputs of instruction tokens after self-attention. Notably, all components of Route-3, including self-attention, cross-attention, and FFN, share parameters with the primary route. Instruction tokens effectively guide object queries and subsequent modules to achieve one-to-many prediction. The shared parameters between the auxiliary and primary routes benefit the one-to-one prediction of the primary route.

Discussion. Large language models have demonstrated impressive capabilities [39] when equipped with meticulously crafted prompts [22, 46]. Subsequent researches treat these prompts as learnable tokens, achieving success in both natural language processing [25, 28, 35] and computer vision applications [23, 51, 66]. While prompt tuning [21, 45, 55] and our proposed instructive self-attention both involve attaching learnable tokens to the input sequence, our instruction token uniquely facilitates distinguishing between one-to-one and one-to-many assignments, rather than merely fine-tuning the model.

Model	w/ Mr. DETR	Epochs	Queries	mAP	AP ₅₀	AP ₇₅	AP _s	AP _m	AP _l
Conditional-DETR [40]		50	300	40.9	61.8	43.3	20.8	44.6	60.2
Anchor-DETR [50]		50	300	42.1	63.1	44.9	22.3	46.2	60.0
SAM-DETR [56]		50	300	39.8	61.8	41.6	20.5	43.4	59.6
DAB-DETR [33]		12	300	44.2	62.5	47.3	27.5	47.1	58.6
DN-DETR [26]		12	300	46.0	63.8	49.9	27.7	49.1	62.3
SQR-DETR [4]		50	300	45.9	64.7	50.2	27.7	49.2	60.5
Deformable DETR++ [67]		12	300	47.0	65.3	51.0	30.1	50.5	60.7
H-DETR [20]		12	300	48.7	66.4	52.9	31.2	51.5	63.5
MS-DETR [62]		12	300	48.8	66.2	53.2	31.5	52.3	63.7
Deformable-DETR++ [67]	✓	12	300	49.5 (+2.5)	67.0	53.7	32.1	52.5	64.7
H-DETR [20]	✓	12	300	49.8 (+1.1)	67.3	54.5	31.6	53.0	65.6
Deformable-DETR++ [67]		12	900	47.6	65.8	51.8	31.2	50.6	62.6
DINO-DETR [58]		12	900	49.0	66.6	53.5	32.0	52.3	63.0
MS-DETR [62]		12	900	50.0	67.3	54.4	31.6	53.2	64.0
DAC-DETR [19]		12	900	49.3	66.5	53.8	31.4	52.4	64.1
Deformable-DETR++ [67]	✓	12	900	50.7 (+3.1)	68.2	55.4	33.6	54.3	64.6
Deformable-DETR++ [67]		24	900	49.8	67.0	54.2	31.4	52.8	64.1
DINO-DETR [58]		24	900	50.4	68.3	54.8	33.3	53.7	64.8
MS-DETR [62]		24	900	50.9	68.4	56.1	34.7	54.3	65.1
DAC-DETR [19]		24	900	50.5	67.9	55.2	33.2	53.5	64.8
Deformable-DETR++ [67]	✓	24	900	51.4 (+1.6)	69.0	56.2	34.9	54.8	66.0
DINO [58]		12	900	49.0	66.6	53.5	32.0	52.3	63.0
Saliency-DETR [17]		12	900	49.2	67.1	53.8	32.7	53.0	63.1
Group-DETR [5]		12	900	49.8	-	-	32.4	53.0	64.2
MS-DETR [62]		12	900	50.3	67.4	55.1	32.7	54.0	64.6
DAC-DETR [19]		12	900	50.0	67.6	54.7	32.9	53.1	64.2
Cascade-DETR [54]		12	900	49.7	67.1	54.1	32.4	53.5	65.1
Align-DETR [1]		12	900	50.2	67.8	54.4	32.9	53.3	65.0
Rank-DETR [42]		12	900	50.4	67.9	55.2	33.6	53.8	64.2
Stable-DINO [34]		12	900	50.4	67.4	55.0	32.9	54.0	65.5
EASE-DETR [13]		12	900	49.7	67.5	54.3	32.7	52.9	64.1
DINO [58]	✓	12	900	50.9 (+1.9)	68.4	55.6	34.6	53.8	65.2
Align-DETR [1]	✓	12	900	51.4 (+1.2)	68.6	55.7	33.8	54.7	66.3
DINO [58]		24	900	50.4	68.3	54.8	33.3	53.7	64.8
Align-DETR [1]		24	900	51.3	68.2	56.1	35.5	55.1	65.6
MS-DETR [62]		24	900	51.7	68.7	56.5	34.0	55.4	65.5
DDQ-DETR [61]		24	900	52.0	69.5	57.2	35.2	54.9	65.9
Stable-DINO [34]		24	900	51.5	68.5	56.3	35.2	54.7	66.5
DAC-DETR [19]		24	900	51.2	68.9	56.0	34.0	54.6	65.4
Align-DETR [1]	✓	24	900	52.3 (+1.0)	69.5	56.7	35.2	56.0	67.0

Table 2. The performance on the COCO 2017 [31] validation set. All models are based on the ResNet-50 [16] backbone.

4. Experiments

4.1. Setup

Dataset and Evaluation. The COCO 2017 dataset [31], widely utilized for object detection and instance segmentation, serves as the benchmark for our model evaluation. In line with existing research [20, 58, 67], we conduct evaluations on the COCO 2017 validation set, providing results in terms of standardized metrics, namely average precision (mAP, AP₅₀, AP₇₅) at various IoU thresholds. AP_s, AP_m, and AP_l refer to the average precision for small, medium,

and large objects, respectively. For all experiments with 300 and 900 queries, we evaluate the performance according to top-100 and top-300 predictions, respectively.

Implement Details. We conduct all experiments based on the ResNet-50 [16] and Swin-L [37] as the backbone pre-trained on the ImageNet [10]. In all experiments, we apply the same data augmentations as [19, 20, 58, 62, 67]. AdamW [38] is employed as the optimizer, with the initial learning rate and weight decay established at 2e-4 and 1e-4, respectively. We utilize a batch size of 16 for training all the models. During training schedules of 12 and 24 epochs,

Model	Epochs	Queries	mAP	AP ₅₀	AP ₇₅	AP _s	AP _m	AP _l
H-DETR [20]	12	300	55.9	75.2	61.0	39.1	59.9	72.2
DINO [58]	12	900	56.8	75.4	62.3	41.1	60.6	73.5
Co-DETR [68]	12	900	56.9	75.5	62.6	40.1	61.2	73.3
Saliency-DETR [17]	12	900	56.5	75.0	61.5	40.2	61.2	72.8
Rank-DETR [42]	12	900	57.6	76.0	63.4	41.6	61.4	73.8
DAC-DETR [19]	12	900	57.3	75.7	62.7	40.1	61.5	74.4
EASE-DETR [13]	12	900	57.8	76.7	63.3	40.7	61.9	73.7
Stable-DINO [34]	12	900	57.7	75.7	63.4	39.8	62.0	74.7
Relation-DETR [18]	12	900	57.8	76.1	62.9	41.2	62.1	74.4
Mr. DETR (ours)	12	900	58.4	76.3	63.9	40.8	62.8	75.3

Table 3. **The performance on the COCO 2017 [31] validation set.** All models are based on the Swin-L [37] backbone.

the learning rate is reduced by a factor of 0.1 following the 11th and 20th epochs, respectively. Within the one-to-many assigner, the hyper-parameters are configured as follows: $K = 6$, $\alpha = 0.3$, and $\tau = 0.4$. In all experiments with instructive self-attention, we set the number of instruction tokens as 10. For models based on DINO [58], we use 100 contrastive denoising queries.

4.2. Main Results

We conduct extensive experiments on the COCO 2017 dataset. In Tab. 2, we present the performance of our method across various baselines, including Deformable-DETR++ [67] with either 300 or 900 queries, DINO [58] and Align-DETR [1]. Specifically, using Deformable-DETR++ [67] with 300 queries, our method achieves a 49.5% mAP, providing a 2.5% improvement without additional inference cost. It surpasses other variants, such as H-DETR [20], MS-DETR [62] and DAC-DETR [19], by approximately 0.7% in mAP. Based on a strong baseline model like Deformable-DETR++ [67] with 900 queries, our multi-route training method reaches a 50.7% mAP under a 12-epoch training schedule. Extending to 24 epochs, our approach enables Deformable-DETR++ [67] to achieve a 51.4% mAP, outperforming the baseline by 1.6%. Compared to other variants with one-to-many auxiliary training, our method exceeds DAC-DETR [19] and MS-DETR [62] by 0.9% and 0.5%, respectively.

Using our approach, DINO baseline [58] can reach 50.9% mAP over 12 epochs, outperforming variants like Group-DETR [5], DAC-DETR [19] and MS-DETR [62]. Previous studies [1, 13, 18, 34, 42, 54] enhance model architectures or implement IoU-aware losses, such as VFL loss [57] and IA-BCE loss [1]. To demonstrate our method’s compatibility with these advancements, we apply it to Align-DETR [1], achieving gains of 1.2% and 1.0% mAP in 12 and 24 epoch schedules, respectively. Our experiments consistently demonstrate improvements across different baseline models. Further experiments with the Swin-L [37] backbone, as shown in Tab. 3, reveal that our method achieves a 58.4% mAP in a 12-epoch training schedule, surpassing other vari-

Epochs	w/ Mr. DETR	Mask mAP	Box mAP
12		32.4	46.5
12	✓	36.0 (+3.6)	49.5 (+3.0)
24		35.1	48.6
24	✓	37.6 (+2.5)	50.3 (+1.7)

Table 4. **Instance segmentation results on the COCO 2017 [31] validation set.** All experiments are based on Deformable-DETR++ [67] with 300 queries and ResNet-50 [16] as backbone.

ants. These experimental results underscore the effectiveness of our proposed method.

4.3. Extension to Instance Segmentation

We integrate our method with the detection transformer architecture for the instance segmentation task. Specifically, following [62, 67], we develop an object mask prediction head based on Deformable-DETR++ [67] utilizing 300 queries. For simplicity, both one-to-one and one-to-many assignments consider only box and classification costs, consistent with the detection transformer. We present the AP metric for both box and mask predictions in Tab. 4. Over a training schedule of 12 and 24 epochs, our auxiliary training method enhances the mask AP by approximately 3.6% and 2.5% compared to the baseline model, respectively. These experimental results highlight the effectiveness of our method.

4.4. Effectiveness Analysis

The parameters of the primary route for one-to-one prediction benefit from auxiliary route training with one-to-many predictions. Recent works [19, 20, 62] demonstrate that incorporating one-to-many assignment as auxiliary training enhances the localization quality of predictions. In this section, we focus on instructive self-attention and examine its role in informing object queries for one-to-many predictions. As illustrated in Fig. 6, we train Deformable-DETR++ [67] with our proposed multi-route approach and visualize the attention map within the instructive self-attention across different decoder layers. For visualization, we use 300 object queries and set 10 instruction tokens. Fig. 6 reveals that when

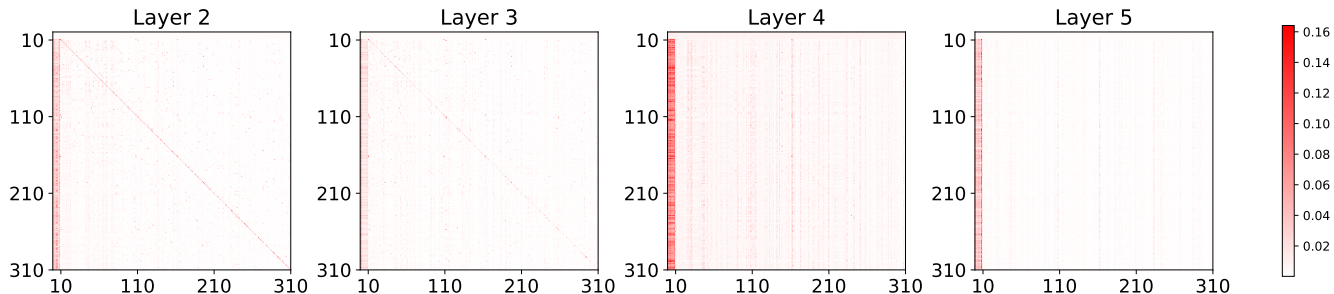


Figure 6. **Visualization of attention maps for instructive self-attention.** We use Deformable-DETR++ with 300 object queries and 10 instruction tokens for this visualization. The first 10 tokens are instruction tokens. The vertical and horizontal axes represent the Query and Key, respectively. Best viewed in PDF with zoom.

Route-1	Route-2	Route-3	mAP	AP ₅₀	AP ₇₅
	✓		47.6	65.8	51.8
✓	✓		49.6 (+2.0)	67.4	54.2
	✓	✓	50.4 (+2.8)	67.9	55.3
✓	✓	✓	50.7 (+3.1)	68.2	55.4

Table 5. **The ablation study of different routes in our method.** ‘Route-1’: the auxiliary training route with independent FFN. ‘Route-2’: the primary route for one-to-one prediction. ‘Route-3’: the auxiliary training route with instructive self-attention.

the 300 object queries act as query and the 10 instruction tokens as key, nearly all 300 object queries exhibit strong activation with the instruction tokens. This indicates that instruction tokens effectively convey information to object queries and subsequent network layers, aiding the model in achieving one-to-many predictions.

4.5. Ablation Study

Effectiveness of Multi-route Training. Our method features a primary route, referred to as Route-2 in Fig. 4, dedicated to one-to-one prediction, and two auxiliary routes, Route-1 and Route-3 for one-to-many prediction. Route-1 utilizes shared self-attention and cross-attention with Route-2, but employs an independent FFN to achieve one-to-many prediction. We introduce an instructive self-attention mechanism in Route-3, which shares all parameters with the primary route. To evaluate the contribution of each auxiliary route, we perform an ablation study, as shown in Tab. 5. Route-1, with its independent FFN, enhances the baseline model by 2.0% mAP. Experimental results indicate that Route-3 provides a 2.8% improvement on Deformable-DETR++ [67], highlighting the effectiveness of our proposed instructive self-attention. By incorporating multi-route training, Deformable-DETR++ [67] achieves 50.7% mAP, surpassing the baseline by 3.1%.

Designs of the Instruction Mechanism. To further reduce the trainable parameters in Route-3 and enhance parameter sharing with the primary route, we introduce the instruction mechanism. In Tab. 6, we evaluate the performance of different designs of the instruction mechanism, as discussed in Sec. 3.3. Initially, we evaluate two conventional variants:

Variants	mAP	AP ₅₀	AP ₇₅
Independent self-attention	50.0	67.7	54.8
Remove self-attention	49.9	67.3	54.7
Independent object queries	49.9	67.5	54.6
Instruction by addition	50.1	67.6	54.7
Instruction by concatenation (ours)	50.7	68.2	55.4

Table 6. **Different designs of instructive self-attention.**

number	1	5	10	50	100
AP	50.2	50.1	50.7	50.4	50.5

(a) The number of instruction tokens.

layers	0	0~1	0~2	0~3	0~4	0~5
AP	50.3	50.2	50.4	50.3	50.4	50.7

(b) Layers of instruction tokens.

Table 7. **Ablation study on configurations of instruction tokens.**

one with independent self-attention and another without self-attention in Route-3. Experimental results indicate that our approach surpasses these variants by 0.7% and 0.8% mAP, respectively. Additionally, we implement a variant using independent object queries in Route-3 while sharing all other parameters with the primary route. Our method exceeds this design by 0.8% mAP. We also investigate an implementation that integrates instruction tokens into the object queries by addition, unlike our method that appends them. Experimental results confirm the superiority of our approach, because it dynamically and flexibly guides the object queries to achieve one-to-many predictions.

Impact of Configurations in Instructive Self-Attention.

We explore different configurations of instruction tokens. First, we examine the impact of varying the number of instruction tokens, as shown in Tab. 7a. The results demonstrate that performance improves with an increased number of instruction tokens. Next, we investigate the effect of incorporating instruction tokens across different decoder layers in Tab. 7b. The experimental results indicate that optimal performance is achieved when all layers utilize instruction tokens. As illustrated in Fig. 6, instruction tokens of all lay-

ers significantly contribute to guiding object queries towards one-to-many targets. In our work, we empirically apply instruction tokens across all six decoder layers and set their number to 10.

5. Conclusion

Regarding the model with auxiliary one-to-many training as a multi-task framework, we examine the roles of each component in the transformer decoder for two training targets. Our empirical findings indicate that any independent component in the decoder can effectively learn both one-to-one and one-to-many training targets, even when other components are shared. Building on this insight, we propose a multi-route training mechanism, featuring a primary route and two auxiliary training routes. This mechanism is further enhanced by our novel instructive self-attention, which dynamically and flexibly guides object queries for one-to-many prediction. Importantly, the auxiliary training routes are discarded during inference, ensuring no impact on model architecture or inference cost. Extensive experiments confirm the effectiveness of our method.

Acknowledgement

This work is supported by Hong Kong Research Grant Council - Early Career Scheme (Grant No. 27208022), National Natural Science Foundation of China (Grant No. 62306251), and HKU Seed Fund for Basic Research. The computations were performed partly using research computing facilities offered by Information Technology Services, the University of Hong Kong.

References

- [1] Zhi Cai, Songtao Liu, Guodong Wang, Zheng Ge, Xiangyu Zhang, and Di Huang. Align-detr: Improving detr with simple iou-aware bce loss. In *Brit. Mach. Vis. Conf.*, 2024. 1, 3, 6, 7
- [2] Xipeng Cao, Peng Yuan, Bailan Feng, and Kun Niu. Cf-detr: Coarse-to-fine transformers for end-to-end object detection. In *AAAI Conf. Artif. Intell.*, 2022. 3
- [3] Nicolas Carion, Francisco Massa, Gabriel Synnaeve, Nicolas Usunier, Alexander Kirillov, and Sergey Zagoruyko. End-to-end object detection with transformers. In *Eur. Conf. Comput. Vis.*, 2020. 1, 3
- [4] Fangyi Chen, Han Zhang, Kai Hu, Yu-Kai Huang, Chenchen Zhu, and Marios Savvides. Enhanced training of query-based object detection via selective query recollection. In *IEEE Conf. Comput. Vis. Pattern Recog.*, 2023. 3, 6
- [5] Qiang Chen, Xiaokang Chen, Jian Wang, Shan Zhang, Kun Yao, Haocheng Feng, Junyu Han, Errui Ding, Gang Zeng, and Jingdong Wang. Group detr: Fast detr training with group-wise one-to-many assignment. In *Int. Conf. Comput. Vis.*, 2023. 1, 3, 6, 7, 17
- [6] Qiang Chen, Xiangbo Su, Xinyu Zhang, Jian Wang, Jiahui Chen, Yunpeng Shen, Chuchu Han, Ziliang Chen, Weixiang Xu, Fanrong Li, et al. Lw-detr: A transformer replacement to yolo for real-time detection. *arXiv preprint arXiv:2406.03459*, 2024. 3
- [7] Zhe Chen, Jing Zhang, and Dacheng Tao. Recurrent glimpse-based decoder for detection with transformer. In *IEEE Conf. Comput. Vis. Pattern Recog.*, 2022. 3
- [8] Yiming Cui, Linjie Yang, and Haichao Yu. Learning dynamic query combinations for transformer-based object detection and segmentation. In *Int. Conf. Mach. Learn.*, 2023. 3
- [9] Xiyang Dai, Yinpeng Chen, Jianwei Yang, Pengchuan Zhang, Lu Yuan, and Lei Zhang. Dynamic detr: End-to-end object detection with dynamic attention. In *Int. Conf. Comput. Vis.*, 2021. 3
- [10] Jia Deng, Wei Dong, Richard Socher, Li-Jia Li, Kai Li, and Li Fei-Fei. Imagenet: A large-scale hierarchical image database. In *IEEE Conf. Comput. Vis. Pattern Recog.*, 2009. 6
- [11] Chengjian Feng, Yujie Zhong, Yu Gao, Matthew R Scott, and Weilin Huang. Tood: Task-aligned one-stage object detection. In *Int. Conf. Comput. Vis.*, 2021. 3
- [12] Peng Gao, Minghang Zheng, Xiaogang Wang, Jifeng Dai, and Hongsheng Li. Fast convergence of detr with spatially modulated co-attention. In *Int. Conf. Comput. Vis.*, 2021. 3
- [13] Yulu Gao, Yifan Sun, Xudong Ding, Chuyang Zhao, and Si Liu. Ease-detr: Easing the competition among object queries. In *IEEE Conf. Comput. Vis. Pattern Recog.*, 2024. 3, 6, 7
- [14] Ziteng Gao, Limin Wang, Bing Han, and Sheng Guo. Adamixer: A fast-converging query-based object detector. In *IEEE Conf. Comput. Vis. Pattern Recog.*, 2022. 3
- [15] Zheng Ge, Songtao Liu, Zeming Li, Osamu Yoshie, and Jian Sun. Ota: Optimal transport assignment for object detection. In *IEEE Conf. Comput. Vis. Pattern Recog.*, 2021. 3
- [16] Kaiming He, Xiangyu Zhang, Shaoqing Ren, and Jian Sun. Deep residual learning for image recognition. In *IEEE Conf. Comput. Vis. Pattern Recog.*, 2016. 6, 7
- [17] Xiuquan Hou, Meiqin Liu, Senlin Zhang, Ping Wei, and Badong Chen. Saliency detr: Enhancing detection transformer with hierarchical saliency filtering refinement. In *IEEE Conf. Comput. Vis. Pattern Recog.*, 2024. 3, 6, 7
- [18] Xiuquan Hou, Meiqin Liu, Senlin Zhang, Ping Wei, Badong Chen, and Xuguang Lan. Relation detr: Exploring explicit position relation prior for object detection. In *Eur. Conf. Comput. Vis.*, 2024. 3, 7
- [19] Zhengdong Hu, Yifan Sun, Jingdong Wang, and Yi Yang. Dac-detr: Divide the attention layers and conquer. *Adv. Neural Inform. Process. Syst.*, 2024. 1, 2, 3, 6, 7, 13, 17, 19
- [20] Ding Jia, Yuhui Yuan, Haodi He, Xiaopei Wu, Haojun Yu, Weihong Lin, Lei Sun, Chao Zhang, and Han Hu. Detr with hybrid matching. In *IEEE Conf. Comput. Vis. Pattern Recog.*, 2023. 1, 3, 6, 7, 13, 17
- [21] Menglin Jia, Luming Tang, Bor-Chun Chen, Claire Cardie, Serge Belongie, Bharath Hariharan, and Ser-Nam Lim. Visual prompt tuning. In *Eur. Conf. Comput. Vis.*, 2022. 5
- [22] Zhengbao Jiang, Frank F Xu, Jun Araki, and Graham Neubig. How can we know what language models know? *Trans. Assoc. Comput. Linguist.*, 2020. 5
- [23] Chen Ju, Tengda Han, Kunhao Zheng, Ya Zhang, and Weidi Xie. Prompting visual-language models for efficient video understanding. In *Eur. Conf. Comput. Vis.*, 2022. 5

- [24] Harold W Kuhn. The hungarian method for the assignment problem. *Naval Res. Logist.*, 1955. 3
- [25] Brian Lester, Rami Al-Rfou, and Noah Constant. The power of scale for parameter-efficient prompt tuning. In *Conf. Empir. Methods Nat. Lang. Process.*, 2021. 5
- [26] Feng Li, Hao Zhang, Shilong Liu, Jian Guo, Lionel M Ni, and Lei Zhang. Dn-detr: Accelerate detr training by introducing query denoising. In *IEEE Conf. Comput. Vis. Pattern Recog.*, 2022. 1, 3, 6
- [27] Feng Li, Ailing Zeng, Shilong Liu, Hao Zhang, Hongyang Li, Lei Zhang, and Lionel M Ni. Lite detr: An interleaved multi-scale encoder for efficient detr. In *IEEE Conf. Comput. Vis. Pattern Recog.*, 2023. 3
- [28] Xiang Lisa Li and Percy Liang. Prefix-tuning: Optimizing continuous prompts for generation. In *Annu. Meet. Assoc. Comput. Linguist.*, 2021. 5
- [29] Yanghao Li, Hanzi Mao, Ross Girshick, and Kaiming He. Exploring plain vision transformer backbones for object detection. In *Eur. Conf. Comput. Vis.*, 2022. 3
- [30] Junyu Lin, Xiaofeng Mao, Yuefeng Chen, Lei Xu, Yuan He, and Hui Xue. D² detr: Decoder-only detr with computationally efficient cross-scale attention. *arXiv preprint arXiv:2203.00860*, 2022. 3
- [31] Tsung-Yi Lin, Michael Maire, Serge Belongie, James Hays, Pietro Perona, Deva Ramanan, Piotr Dollár, and C Lawrence Zitnick. Microsoft coco: Common objects in context. In *Eur. Conf. Comput. Vis.*, 2014. 6, 7
- [32] Tsung-Yi Lin, Priya Goyal, Ross B. Girshick, Kaiming He, and Piotr Dollár. Focal loss for dense object detection. *Int. Conf. Comput. Vis.*, 2017. 1, 3
- [33] Shilong Liu, Feng Li, Hao Zhang, Xiao Yang, Xianbiao Qi, Hang Su, Jun Zhu, and Lei Zhang. Dab-detr: Dynamic anchor boxes are better queries for detr. In *Int. Conf. Learn. Represent.*, 2022. 1, 3, 6
- [34] Shilong Liu, Tianhe Ren, Jiayu Chen, Zhaoyang Zeng, Hao Zhang, Feng Li, Hongyang Li, Jun Huang, Hang Su, Jun Zhu, et al. Detection transformer with stable matching. In *Int. Conf. Comput. Vis.*, 2023. 3, 6, 7
- [35] Xiao Liu, Kaixuan Ji, Yicheng Fu, Weng Lam Tam, Zhengxiao Du, Zhilin Yang, and Jie Tang. P-tuning v2: Prompt tuning can be comparable to fine-tuning universally across scales and tasks. In *Annu. Meet. Assoc. Comput. Linguist.*, 2022. 5
- [36] Yang Liu, Yao Zhang, Yixin Wang, Yang Zhang, Jiang Tian, Zhongchao Shi, Jianping Fan, and Zhiqiang He. Sap-detr: bridging the gap between salient points and queries-based transformer detector for fast model convergence. In *IEEE Conf. Comput. Vis. Pattern Recog.*, 2023. 3
- [37] Ze Liu, Yutong Lin, Yue Cao, Han Hu, Yixuan Wei, Zheng Zhang, Stephen Lin, and Baining Guo. Swin transformer: Hierarchical vision transformer using shifted windows. In *Int. Conf. Comput. Vis.*, 2021. 6, 7, 18
- [38] Ilya Loshchilov and Frank Hutter. Decoupled weight decay regularization. In *Int. Conf. Learn. Represent.*, 2017. 6
- [39] Ben Mann, N Ryder, M Subbiah, J Kaplan, P Dhariwal, A Neelakantan, P Shyam, G Sastry, A Askell, S Agarwal, et al. Language models are few-shot learners. *arXiv preprint arXiv:2005.14165*, 2020. 5
- [40] Depu Meng, Xiaokang Chen, Zejia Fan, Gang Zeng, Houqiang Li, Yuhui Yuan, Lei Sun, and Jingdong Wang. Conditional detr for fast training convergence. In *Int. Conf. Comput. Vis.*, 2021. 1, 3, 6
- [41] Jeffrey Ouyang-Zhang, Jang Hyun Cho, Xingyi Zhou, and Philipp Krähenbühl. Nms strikes back. *arXiv preprint arXiv:2212.06137*, 2022. 1, 3, 19
- [42] Yifan Pu, Weicong Liang, Yiduo Hao, Yuhui Yuan, Yukang Yang, Chao Zhang, Han Hu, and Gao Huang. Rank-detr for high quality object detection. *Adv. Neural Inform. Process. Syst.*, 2024. 3, 6, 7
- [43] Shaoqing Ren, Kaiming He, Ross Girshick, and Jian Sun. Faster r-cnn: Towards real-time object detection with region proposal networks. *IEEE Trans. Pattern Anal. Mach. Intell.*, 2016. 1, 3
- [44] Byungseok Roh, JaeWoong Shin, Wuhyun Shin, and Saehoon Kim. Sparse detr: Efficient end-to-end object detection with learnable sparsity. In *Int. Conf. Learn. Represent.*, 2022. 3
- [45] Sheng Shen, Shijia Yang, Tianjun Zhang, Bohan Zhai, Joseph E Gonzalez, Kurt Keutzer, and Trevor Darrell. Multitask vision-language prompt tuning. In *IEEE Winter Conf. Appl. Comput. Vis.*, 2024. 5
- [46] Taylor Shin, Yasaman Razeghi, Robert L Logan IV, Eric Wallace, and Sameer Singh. Autoprompt: Eliciting knowledge from language models with automatically generated prompts. *arXiv preprint arXiv:2010.15980*, 2020. 5
- [47] Zhiqing Sun, Shengcao Cao, Yiming Yang, and Kris M Kitani. Rethinking transformer-based set prediction for object detection. In *Int. Conf. Comput. Vis.*, 2021. 1, 2, 3
- [48] Yao Teng, Haisong Liu, Sheng Guo, and Limin Wang. Stageinteractor: Query-based object detector with cross-stage interaction. In *Int. Conf. Comput. Vis.*, 2023. 3
- [49] Zhi Tian, Chunhua Shen, Hao Chen, and Tong He. Fcos: A simple and strong anchor-free object detector. *IEEE Trans. Pattern Anal. Mach. Intell.*, 2020. 1, 3
- [50] Yingming Wang, Xiangyu Zhang, Tong Yang, and Jian Sun. Anchor detr: Query design for transformer-based detector. In *AAAI Conf. Artif. Intell.*, 2022. 1, 3, 6
- [51] Zifeng Wang, Zizhao Zhang, Chen-Yu Lee, Han Zhang, Ruoxi Sun, Xiaoqi Ren, Guolong Su, Vincent Perot, Jennifer Dy, and Tomas Pfister. Learning to prompt for continual learning. In *IEEE Conf. Comput. Vis. Pattern Recog.*, 2022. 5
- [52] Chenhongyi Yang, Zehao Huang, and Naiyan Wang. Query-det: Cascaded sparse query for accelerating high-resolution small object detection. In *IEEE Conf. Comput. Vis. Pattern Recog.*, 2022. 3
- [53] Zhuyu Yao, Jiangbo Ai, Boxun Li, and Chi Zhang. Efficient detr: improving end-to-end object detector with dense prior. *arXiv preprint arXiv:2104.01318*, 2021. 3
- [54] Mingqiao Ye, Lei Ke, Siyuan Li, Yu-Wing Tai, Chi-Keung Tang, Martin Danelljan, and Fisher Yu. Cascade-detr: delving into high-quality universal object detection. In *Int. Conf. Comput. Vis.*, 2023. 3, 6, 7
- [55] Seungryoung Yoo, Eunji Kim, Dahyun Jung, Jungbeom Lee, and Sungroh Yoon. Improving visual prompt tuning for self-supervised vision transformers. In *Int. Conf. Mach. Learn.*, 2023. 5

- [56] Gongjie Zhang, Zhipeng Luo, Yingchen Yu, Kaiwen Cui, and Shijian Lu. Accelerating detr convergence via semantic-aligned matching. In *IEEE Conf. Comput. Vis. Pattern Recog.*, 2022. 3, 6
- [57] Haoyang Zhang, Ying Wang, Feras Dayoub, and Niko Sunderhauf. Varifocalnet: An iou-aware dense object detector. In *IEEE Conf. Comput. Vis. Pattern Recog.*, 2021. 7
- [58] Hao Zhang, Feng Li, Shilong Liu, Lei Zhang, Hang Su, Jun Zhu, Lionel Ni, and Heung-Yeung Shum. Dino: Detr with improved denoising anchor boxes for end-to-end object detection. In *Int. Conf. Learn. Represent.*, 2023. 1, 3, 6, 7, 13, 18
- [59] Manyuan Zhang, Guanglu Song, Yu Liu, and Hongsheng Li. Decoupled detr: Spatially disentangling localization and classification for improved end-to-end object detection. In *Int. Conf. Comput. Vis.*, 2023. 3
- [60] Shifeng Zhang, Cheng Chi, Yongqiang Yao, Zhen Lei, and Stan Z Li. Bridging the gap between anchor-based and anchor-free detection via adaptive training sample selection. In *IEEE Conf. Comput. Vis. Pattern Recog.*, 2020. 3
- [61] Shilong Zhang, Xinjiang Wang, Jiaqi Wang, Jiangmiao Pang, Chengqi Lyu, Wenwei Zhang, Ping Luo, and Kai Chen. Dense distinct query for end-to-end object detection. In *IEEE Conf. Comput. Vis. Pattern Recog.*, 2023. 3, 6
- [62] Chuyang Zhao, Yifan Sun, Wenhao Wang, Qiang Chen, Errui Ding, Yi Yang, and Jingdong Wang. Ms-detr: Efficient detr training with mixed supervision. In *IEEE Conf. Comput. Vis. Pattern Recog.*, 2024. 1, 2, 3, 6, 7, 13, 17, 19
- [63] Jinjing Zhao, Fangyun Wei, and Chang Xu. Hybrid proposal refiner: Revisiting detr series from the faster r-cnn perspective. In *IEEE Conf. Comput. Vis. Pattern Recog.*, 2024. 3
- [64] Yian Zhao, Wenyu Lv, Shangliang Xu, Jinman Wei, Guanzhong Wang, Qingqing Dang, Yi Liu, and Jie Chen. Detsr beat yolos on real-time object detection. In *IEEE Conf. Comput. Vis. Pattern Recog.*, 2024. 3
- [65] Ge Zheng, Liu Songtao, Wang Feng, Li Zeming, Sun Jian, et al. YOLOX: Exceeding yolo series in 2021. *arXiv preprint arXiv:2107.08430*, 2021. 3
- [66] Kaiyang Zhou, Jingkang Yang, Chen Change Loy, and Ziwei Liu. Learning to prompt for vision-language models. *Int. J. Comput. Vis.*, 2022. 5
- [67] Xizhou Zhu, Weijie Su, Lewei Lu, Bin Li, Xiaogang Wang, and Jifeng Dai. Deformable detr: Deformable transformers for end-to-end object detection. In *Int. Conf. Learn. Represent.*, 2021. 1, 3, 6, 7, 8, 13, 14, 15, 16, 17
- [68] Zhuofan Zong, Guanglu Song, and Yu Liu. Detsr with collaborative hybrid assignments training. In *Int. Conf. Comput. Vis.*, 2023. 3, 7

A. Pseudo-Code for Instructive Self-Attention

We present the PyTorch-style pseudo-code for our proposed instructive self-attention method in Alg. 1. As detailed in our primary manuscript, our multi-route training approach involves three training routes. Route-2 serves as the primary route designated for one-to-one prediction, which is the same as the baseline model. Route-1 acts as an auxiliary route with an independent FFN aimed at one-to-many predictions. Meanwhile, Route-3 operates as an auxiliary route incorporating our novel instructive self-attention to facilitate one-to-many predictions. In this approach, we establish a collection of trainable tokens as instructions to direct the object queries and subsequent modules in executing one-to-many prediction. These trainable instruction tokens are affixed to the input object queries through concatenation, allowing for the dynamic and adaptable transmission of instructions via self-attention mechanisms. The resulting output from the instruction tokens after undergoing self-attention is not retained, as these tokens do not possess the capability to locate objects.

Algorithm 1 Pseudo-code of Pooled Cube Distillation in a PyTorch-like style.

```
class InstructAttn(nn.Module):
    def __init__(self, embed_dim, num_heads, num_ins):
        # embed_dim: the embedding dimension used
        # num_heads: the number of heads in self-attention
        # num_ins: the number of instruction tokens
        self.ins_sa = nn.MultiheadAttention(
            embed_dim = embed_dim,
            num_heads = num_heads,
        )

        # define learnable instruction tokens
        self.instruct_o2m = nn.Embedding(num_ins, embed_dim)
        self.pos_o2m = nn.Embedding(num_ins, embed_dim)
        self.num_ins = num_ins

    def forward(self, query, key, value, query_pos, key_pos, route="route-3"):
        # route: identify the current route
        query = query + query_pos
        key = key + key_pos
        if mode == "route-3":
            ins_token = self.instruct_o2m.weight
            ins_pos = self.pos_o2m.weight

            # concatenate instruction tokens into the input sequence
            query = torch.cat([ins_token + ins_pos, query], dim=1)
            key = torch.cat([ins_token + ins_pos, key], dim=1)
            value = torch.cat([ins_token, value], dim=1)

        # perform self-attention
        out = self.ins_sa(
            query, key, value
        )
        if mode == "route-3":
            # discard the corresponding output of instruction tokens
            out = out[:, self.num_ins:, :]
        return out
```

B. Convergence Curves

Employing Deformable-DETR++ [67] with 300 queries, we perform training on the instance segmentation task both with and without the integration of our proposed approach. Consistent with established methods [19, 20, 58, 62, 67], models are trained using 12 and 24 epoch schedules, respectively. The learning rate is reduced by a factor of 0.1 at the 11th and 20th epochs according to the 12 and 24 epoch schedules, respectively. We illustrate the evaluation results for bounding box predictions in Fig. 7(a) and for instance mask predictions in Fig. 7(b). The evaluation results demonstrate that our approach significantly enhances the training process of the baseline model.

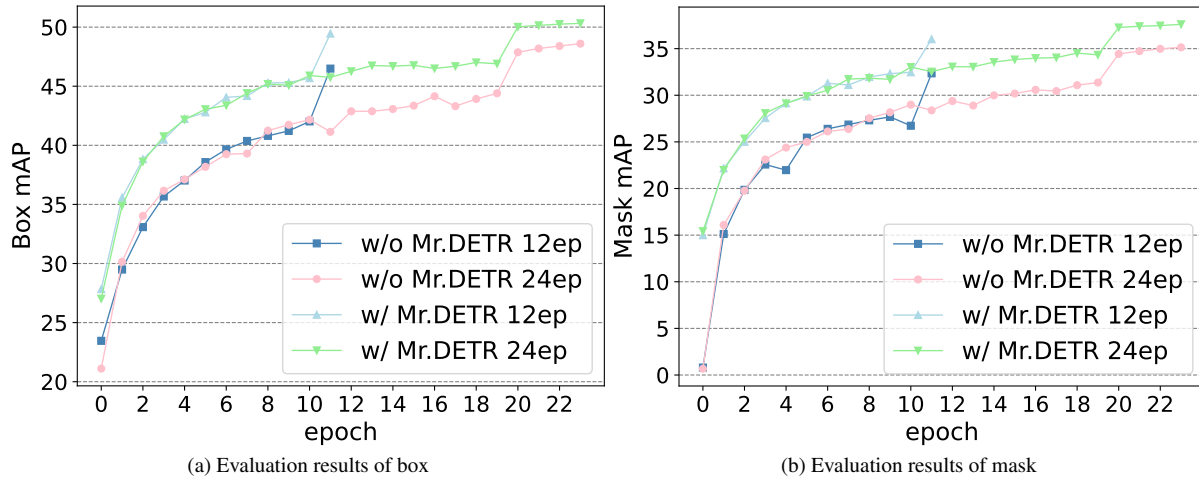


Figure 7. **Evaluation results of each epoch.** We utilize the Deformable-DETR++ (300 queries) as the baseline model, which is trained for 12 and 24 epochs, respectively.

C. Detailed Performance of Each Route

As detailed in Sec. B, we train Mr. DETR for the instance segmentation task based on Deformable-DETR++ [67]. We report the evaluation results of each route of our method in Tab. 8. Experimental results indicate that the primary route is adept at accomplishing one-to-one prediction, as evidenced by the fact that Non-Maximum-Suppression (NMS) yields only a minor improvement of approximately 0.1 - 0.2% in both box mAP and mask mAP. Conversely, for the auxiliary routes, the application of NMS significantly improves the performance (about 35% and 25% in terms of box mAP and mask mAP) of Route-1 and Route-3, highlighting their capability for effective one-to-many prediction. This further substantiates that our introduced instructive self-attention is proficient in efficiently guiding object queries for one-to-many prediction.

Route	Epoch	NMS	Box						Mask					
			mAP	AP ₅₀	AP ₇₅	AP _s	AP _m	AP _l	mAP	AP ₅₀	AP ₇₅	AP _s	AP _m	AP _l
Baseline	12		46.5	64.2	50.8	28.8	50.0	60.7	32.4	55.7	32.6	11.9	35.6	54.4
Baseline	12	✓	46.7	65.0	50.7	29.0	50.1	60.9	32.5	56.3	32.6	12.0	35.8	54.8
Route-2 (primary)	12		49.5	66.6	54.1	30.3	52.6	64.7	36.0	59.8	37.2	13.6	39.6	59.7
Route-2 (primary)	12	✓	49.7	67.6	54.1	30.4	52.8	65.0	36.2	60.5	37.2	13.7	39.8	60.1
Route-1 (auxiliary)	12		14.5	18.8	16.0	15.6	21.6	19.1	10.9	17.1	11.6	5.9	13.4	20.2
Route-1 (auxiliary)	12	✓	49.8	67.3	54.6	31.0	53.0	65.3	36.1	60.1	37.2	13.9	39.4	59.9
Route-3 (auxiliary)	12		14.5	18.7	15.9	15.3	22.1	19.7	10.8	17.0	11.5	5.6	13.6	20.3
Route-3 (auxiliary)	12	✓	49.9	67.3	54.6	30.8	53.2	65.4	36.2	60.2	37.3	13.6	39.5	59.8
Baseline	24		48.6	66.4	53.1	30.8	51.9	62.9	35.1	59.1	36.0	14.3	38.9	57.5
Baseline	24	✓	48.6	67.1	52.8	30.9	51.8	63.0	35.2	59.6	35.9	14.4	39.0	57.7
Route-2 (primary)	24		50.3	68.0	54.7	31.5	53.2	65.0	37.6	61.4	38.9	15.1	41.4	60.5
Route-2 (primary)	24	✓	50.4	68.7	54.6	31.6	53.3	65.2	37.7	61.9	38.9	15.1	41.6	60.9
Route-1 (auxiliary)	24		14.0	18.1	15.2	15.4	21.1	18.4	10.7	16.6	11.3	5.8	13.4	19.1
Route-1 (auxiliary)	24	✓	50.4	68.2	55.1	31.5	53.5	65.2	37.6	61.7	38.8	14.9	41.2	60.4
Route-3 (auxiliary)	24		14.1	18.3	15.3	15.6	21.2	18.8	10.7	16.7	11.3	5.9	13.3	19.3
Route-3 (auxiliary)	24	✓	50.4	68.2	54.8	31.7	53.4	65.2	37.6	61.6	38.8	14.9	41.2	60.5

Table 8. **The detailed performance of each route in Mr. DETR.** The Deformable-DETR++ [67] employing 300 queries serves as our baseline model. ‘Route-2’: the primary route employed for one-to-one prediction, identical in functionality to the baseline model. ‘Route-1’: the auxiliary route for one-to-many prediction, which is built with an independent FFN. ‘Route-3’: the auxiliary route for one-to-many prediction, which utilizes our proposed instructive self-attention.

D. Detailed Performance of Intermediate Layers

Typically, DETR-like object detectors consist of six layers each in their transformer encoders and decoders. As mentioned in Sec. B and Sec. C, our approach for mask prediction is based on Deformable-DETR++ [67], utilizing solely the last decoder layer. All six decoder layers are employed for object detection tasks. Therefore, we only evaluate the box prediction for all layers as shown in Tab. 9. Evaluation results suggest that our method can effectively improve the performance of the primary route across all six decoder layers, demonstrating the efficacy of our approach. Moreover, the one-to-many prediction training routes, namely, Route-1 and Route-3, significantly surpass the primary route in the shallower layers. For example, with a model trained on a 12-epoch schedule, Route-3 achieves a 6.4% improvement over the primary route in layer 0, and a 0.4% improvement in layer 5. These experiments indicate that the primary route needs more decoder layers to reach comparable performance as the auxiliary routes equipped with NMS. For instance, Route-1 and Route-3 can reach 49.4% mAP in layer 2, while the primary route achieves 49.4% mAP in layer 4.

Method	Layer	Route	Epoch	NMS	mAP	AP ₅₀	AP ₇₅	AP _s	AP _m	AP _l
Baseline [67]	0	-	12		38.5	53.4	42.2	23.1	41.8	50.0
w/ Mr.DETR	0	Route-2			41.0 (+2.5)	55.5	45.0	24.8	43.8	54.3
w/ Mr.DETR	0	Route-1		✓	47.5	64.9	52.2	29.0	51.0	62.1
w/ Mr.DETR	0	Route-3		✓	47.4	64.9	52.3	29.1	50.9	62.4
Baseline [67]	1	-	12		42.6	58.7	46.5	25.7	46.2	55.1
w/ Mr.DETR	1	Route-2			45.8 (+3.2)	61.8	50.3	27.6	49.0	60.3
w/ Mr.DETR	1	Route-1		✓	48.9	66.1	53.5	30.4	52.4	63.8
w/ Mr.DETR	1	Route-3		✓	49.0	66.3	53.6	30.4	52.6	64.2
Baseline [67]	2	-	12		45.0	62.0	49.2	27.7	48.7	58.6
w/ Mr.DETR	2	Route-2			48.0 (+3.0)	64.7	52.5	29.3	51.3	62.4
w/ Mr.DETR	2	Route-1		✓	49.4	66.7	54.2	31.1	52.8	64.3
w/ Mr.DETR	2	Route-3		✓	49.4	66.5	54.1	31.0	52.8	64.3
Baseline [67]	3	-	12		46.1	63.5	50.4	28.6	49.6	60.1
w/ Mr.DETR	3	Route-2			49.0 (+2.9)	66.0	53.5	30.4	52.3	63.7
w/ Mr.DETR	3	Route-1		✓	49.7	67.1	54.5	31.3	53.0	64.8
w/ Mr.DETR	3	Route-3		✓	49.9	67.2	54.6	31.4	53.3	64.8
Baseline [67]	4	-	12		46.4	64.1	50.7	29.0	50.0	60.7
w/ Mr.DETR	4	Route-2			49.4 (+3.0)	66.5	54.0	30.4	52.6	64.3
w/ Mr.DETR	4	Route-1		✓	49.9	67.4	54.7	31.1	53.2	65.3
w/ Mr.DETR	4	Route-3		✓	50.0	67.5	54.7	31.3	53.3	65.7
Baseline [67]	5	-	12		46.5	64.2	50.8	28.8	50.0	60.7
w/ Mr.DETR	5	Route-2			49.5 (+3.0)	66.6	54.1	30.3	52.6	64.7
w/ Mr.DETR	5	Route-1		✓	49.8	67.3	54.6	31.0	53.0	65.3
w/ Mr.DETR	5	Route-3		✓	49.9	67.3	54.6	30.8	53.2	65.4
Baseline [67]	0	-	24		41.3	56.3	45.4	25.5	44.6	53.2
w/ Mr.DETR	0	Route-2			42.6 (+1.3)	57.3	46.4	25.8	44.8	55.9
w/ Mr.DETR	0	Route-1		✓	48.2	65.8	52.7	29.1	51.4	62.5
w/ Mr.DETR	0	Route-3		✓	48.2	66.0	52.8	29.2	51.6	62.2
Baseline [67]	1	-	24		45.1	61.5	49.5	28.2	48.3	58.1
w/ Mr.DETR	1	Route-2			47.1 (+2.0)	63.3	51.3	28.4	49.9	61.2
w/ Mr.DETR	1	Route-1		✓	49.6	67.1	54.2	30.5	52.9	63.9
w/ Mr.DETR	1	Route-3		✓	49.7	67.3	54.2	30.6	53.0	64.1
Baseline [67]	2	-	24		47.2	64.3	51.8	29.8	50.3	60.8
w/ Mr.DETR	2	Route-2			49.2 (+2.0)	66.2	53.6	30.2	52.2	63.4
w/ Mr.DETR	2	Route-1		✓	50.1	67.7	54.8	31.1	53.3	64.8
w/ Mr.DETR	2	Route-3		✓	50.2	67.9	54.7	31.4	53.5	64.7
Baseline [67]	3	-	24		48.1	65.7	52.7	30.8	51.3	61.8
w/ Mr.DETR	3	Route-2			50.0 (+1.9)	67.4	54.4	30.9	53.0	64.5
w/ Mr.DETR	3	Route-1		✓	50.2	68.0	54.8	31.7	53.4	64.8
w/ Mr.DETR	3	Route-3		✓	50.3	68.1	54.8	31.5	53.4	65.0
Baseline [67]	4	-	24		48.6	66.3	53.1	30.9	51.8	62.3
w/ Mr.DETR	4	Route-2			50.3 (+1.7)	67.9	54.7	31.3	53.2	65.0
w/ Mr.DETR	4	Route-1		✓	50.5	68.3	55.1	31.7	53.7	65.1
w/ Mr.DETR	4	Route-3		✓	50.4	68.3	54.9	32.0	53.5	65.3
Baseline [67]	5	-	24		48.6	66.4	53.1	30.8	51.9	62.9
w/ Mr.DETR	5	Route-2			50.3 (+1.7)	68.0	54.7	31.5	53.2	65.0
w/ Mr.DETR	5	Route-1		✓	50.4	68.2	55.1	31.5	53.5	65.2
w/ Mr.DETR	5	Route-3		✓	50.4	68.2	54.8	31.7	53.4	65.2

Table 9. Evaluation results of box prediction in all six decoder layers. ‘Route-2’: the primary route for one-to-one prediction. ‘Route-1’: the auxiliary route with an independent FFN. ‘Route-3’: the auxiliary route with an instructive self-attention.

E. Training Cost

We measure the training time of different methods in Tab. 10. The training time denotes the average duration of each epoch. We evaluate training time on 8 NVIDIA 3090 GPUs with a batch size of 16. The experimental results indicate that our proposed method achieves an effective trade-off between performance and training time.

Model	Training Time (minutes)	mAP
Deformable-DETR++ [67]	84	47.0
H-DETR [20]	104 (+20)	48.7 (+1.7)
DAC-DETR [19]	94 (+10)	-
MS-DETR [62]	96 (+12)	48.8 (+1.8)
Group-DETR [5]	123 (+39)	-
Mr. DETR (Ours)	101 (+17)	49.5 (+2.5)

Table 10. **Comparison of training time of various methods.** All methods utilize Deformable-DETR++ with 300 queries as the baseline. The training time represents the average duration per training epoch.

F. Qualitative Results

We present the prediction results of our method in Fig. 8. The model is based on the DINO [58] baseline with Swin-L [37] backbone.



Figure 8. Qualitative results of our method. Left: prediction results. Right: ground-truth.

G. Impact of Hyper-Parameters

Fig. 9 shows the influence of the hyper-parameters K , α , and τ in the one-to-many assignment [19, 41, 62]. In Fig. 9a, we observe that as the number of positive candidates increases, the model achieves its highest performance when $K = 6$. However, when $K > 7$, the one-to-many assignment increases the difficulty of removing duplicates in the primary route, leading to decreased performance. For the weight of classification confidence α , as shown in Fig. 9b, the model achieves the best performance at $\alpha = 0.3$. Similarly, in Fig. 9c, the performance improves as the filter threshold τ increases, reaching its peak at $\tau = 0.4$. Beyond this value, the performance declines, potentially due to the filtering out of many high-quality candidates. In our method, we empirically set $K = 6$, $\alpha = 0.3$, and $\tau = 0.4$.

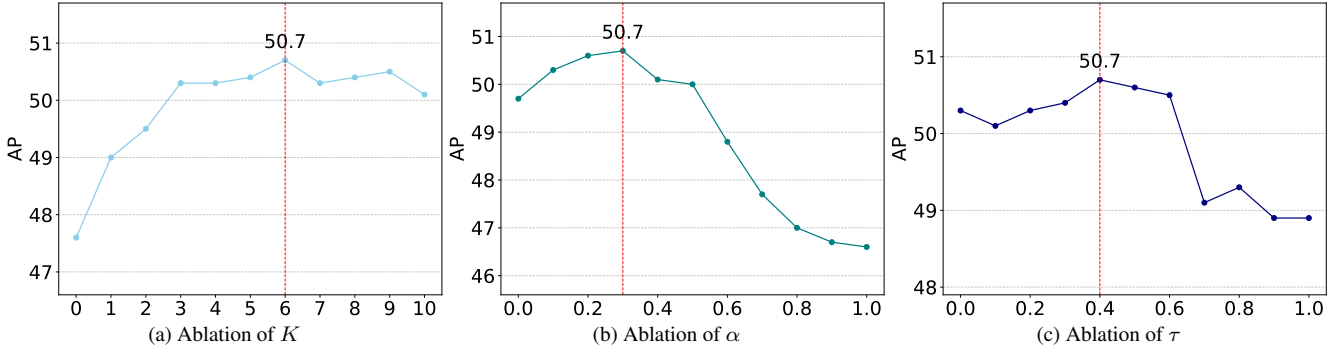


Figure 9. **Influence of hyper-parameters K , α and τ in the one-to-many assignment.** (a) Influence of K for selecting top- K positive candidates. (b) Influence of α that denotes the weight of classification confidence when forming the matching score M . (c) Influence of τ that is used to filter out low-quality candidates.